

A Swift Algorithm and Hue Preserving Based Mechanism for Underwater Image Colour Enhancement

Vishnu Soni¹, Abhay Sharma², Jitendra Rajpurohit³

Submitted: 16/08/2023

Revised: 06/10/2023

Accepted: 20/10/2023

Abstract— Underwater images often exhibit colour variations and poor perceptibility due to wavelength dependent light absorption and scattering. In order to address these problems, we introduce a swift algorithm and hue-preserving based mechanism for an effective and reliable underwater image enhancement. In order to reduce the excessive pixel values, we initially used a simple logarithmic function as a preprocessing step. The brightness and contrast are then altered using a novel nonlinear enhancement operation that was developed empirically on the basis of mathematical, statistical and spatial data. Additionally, as a post-processing step, a regularisation function is used to rearrange image pixels in the natural dynamic range. We also used CHS and WDF techniques which perform on HIS and HSV colour models, respectively. Prior to applying a WDF method to the S and I components, the degraded images are initially transformed from RGB color model to HIS colour model. This model preserves hue component H. The image is then changed in the HSV color model in a similar way, with the H component being kept invariant and the S and V components being process using CHS method. Experimental findings shows that the enhancement of image quality in terms of qualitative and quantitative evaluation in the proposed method. Our method has been demonstrated successfully enhancing underwater images having colour distortion, poor contrast and detail loss.

Keywords— Image enhancement, underwater image, swift algorithm, constrained histogram stretching (CHS), wavelet domain filtering (WDF).

1.Introduction

The advancement of marine resource development, marine biological research, and undersea environmental evaluation is being accelerated by researchers' interest in underwater computer vision technologies. These accomplishments have made it possible for underwater imaging research to have strategic significance and practical application value [1]. However, an imaging component is not able to produce better quality underwater photographs since light is particularly observed by water throughout its propagation and the

scatter by suspended microparticles as shown in Fig.1. The degraded photographs frequently suffered from low contrast and colour cast concerns. Therefore, there is still a need for study in the domain of computer vision to overcome the poor-quality underwater photographs. The target distance as well as underwater depth have an impact on the imaging quality of underwater images. The Jaffe McGlamery underwater optical imaging model considers light source, medium, sensor and object reflection qualities. The three forms of light scattering caused by water in this model are forward, backward and back scattering.

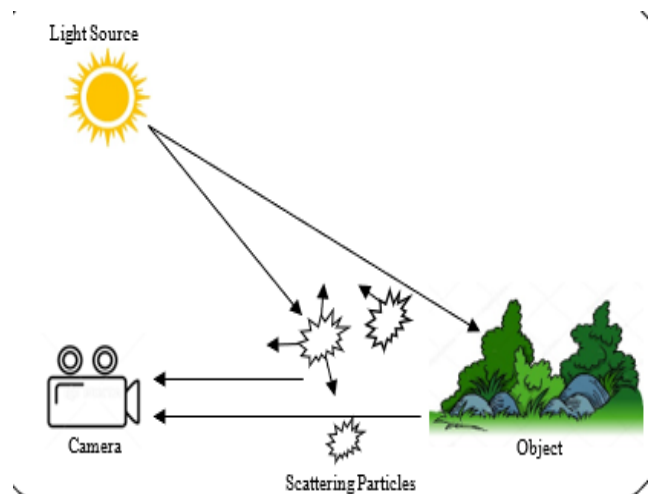


Fig.1. Underwater imaging through a scattering medium [1]

¹Amity University Rajasthan, Jaipur, India

²Manipal University Jaipur, Jaipur, India

³Symbiosis International Deemed University, Pune, India.

Corresponding Author: vishnusoni2221991@gmail.com

abhaysharma2004@gmail.com

jiten_rajpurohit@yahoo.com

These three scattering components are processed as a linear sum to create the total light scattering effect in underwater imaging. The forward scattering is slight angular deviation of the light reflected through water elements during its transmission in the lens. The direct scattering is the scattering of the target items to the imaging system. Details become hazy because the dispersed light's path diverges from its original transmission direction. When light strikes water impurities, it scatters, a phenomenon known as backscattering. Depth and the angle of imaging system as well as the level of colour attenuation of underwater photographs are all affected differently by backscattering. However, the majority of documented underwater photography improvement techniques typically ignore the colour cast quality. Rather, they apply global processing to the whole image where it causes local RGB three-channel region to be overcompensated.

This study develops a novel method for underwater image enhancement using a swift algorithm and hue preserving based mechanism. The key contributions of this study are summarised as follows.

- 1) This study presents a competent image enhancing method by combining the hue saturation intensity (HIS) and hue saturation value (HSV) color models.
- 2) The noncomplex logarithmic function is applied as the preprocessing stage to obtain a reasonable intensity equalisation and remove immoderate pixel values.
- 3) The method used wavelet domain filtering (WDF) and constrained histogram stretching (CHS) schemes operated on HIS and HSV colour models, respectively wherein the hue component (H) is preserved in both operations.
- 4) The experimental findings support the accuracy of the color characteristic analysis, the generalizability of underwater photograph improvement techniques and the viability of underwater imaging improvement in a range of settings. Empirical results assures that the proposed method generates better results than other widely popular underwater enhancement algorithms in terms of both visually and quantitative analysis.

The rest part of this paper is structured as follows. A comprehensive study of related works is presented in Section 2 and Section 3 gives a detailed introduction to the enhancement techniques for underwater imaging including the swift algorithm, colour models and enhancement algorithms. The experimental validation of our strategy and discussion of the qualitative and quantitative evaluation are covered in Section 4. The proposed method is finally summarised in Section 5.

2. Literature Survey

The underwater enhancement methods such as underwater image restoration techniques [3]– [5], underwater image enhancement [6]– [8], and data-driven techniques [9]– [11] has been put forward successively to enhance image quality. To reconstruct high-quality underwater photograph, image restoration methods account for the degraded physical model. Because of the many complicated underwater physical and optical aspects, restoration techniques are not easily adaptable. Without taking underwater imaging parameters into account, enhancement methods concentrate on modifying pixel values to improve underwater images [11]. Even though the enhancement methods are quick and easy, they often over-or under-enhanced because underwater optical imaging parameters are not taken into consideration. Data-driven techniques training is relied on artificial pairs of low- and high-quality images. Though, data driven approaches rely on the large numbers of training data as well as complex network architectures. By reversing the degraded procedures and computing parameters of degraded model, the underwater image restoration strategy aims to restore underwater images. The recovery of underwater images using polarization-based techniques [12], [13] may increase the clarity and contrast of the images. Moreover, to acquire features of deep scene of multiple degrees of polarization, hardware devices are required. The dark channel prior (DCP) [14] has recently proved its dominance in the domain of image enhancement. Other algorithms are utilised for restoring the underwater images [16]– [18]. From the stance of a physical degeneration, Zhou et al. [2] presented a technique on the basis of for removal of color cast and backscatter pixel prior. Backscatter map, illumination map and depth map can all be accurately estimated using this strategy with just single underwater image as an input. In order to enhancing contrast, the backscatter estimation strategy is introduced on the basis of depth map for underwater images. Further on the basis of illumination map, a method is established to eliminate color variations. In precise a color compensation method was developed to totally remove artifacts that have been caused by the robust removal of red channel. An underwater restoration approach on the basis of distribution of information and light scattering prior was presented to solve the degradation concerns [3]. In accordance with the details distributions as well as light scattering attributes of the background light region, it first estimates the background light. The relation between the brightness details as well as color attenuation is then used to achieve scene depth map as well as transmission map. To obtain a restored image,

an underwater image details method is subsequently reversed. To remove color distortion, a method based on scene depth map as well as the color correction technique was put forth [4]. To construct the depth map, this technique first designs a technique for estimating the depth of underwater images. Backscatter is then computed and eliminated by the channel using this model in accordance with depth value of each pixel. A secondary guided transmission map-based technique was put forth that can successfully reconstruct the color, visibility, and authentic appearance of underwater images [17]. The enhancement of transmission map is carried out using optimised guided filtering. After processing the images, a polished transmission map is then restored. The restored image is then subjected to auto level processing to enhance the contrast.

Sharma et al. [16] demonstrates by assigning the proper receptive field size on the basis of traversing range of color channel that could result in a significant performance improvement. This method also incorporated attentive skip operation to iteratively improve learned multi-contextual properties. Feature priors influenced by underwater scene priors were recently proposed [15]. In more detail, this strategy creates a strong model for calculating the background light based on hue, brightness, and flatness feature priors that could efficiently decrease color distortion. The improved contrast is achieved while maintaining edge information with the finely tuned transmission map. By changing the pixel values of images, underwater image enhancing approach could improve the contrast and brightness. It mostly consists of histogram based [19]– [21], Retinex-based [22]– [24], and fusion-based [25]. To enhance the visual quality while improving contrast, Ulutas et al. [5] combines local as well as global contrast enhancing techniques. Meanwhile local technique takes into consideration the local brightness properties, global technique guarantees the complete enhancing of image. Local color correction is also used on underwater images using this technique. This technique splits photograph into non-over-lapping sub blocks and employ histogram to them whereas methods in the literature used numerous methods to the global histogram of channels. The technique corrects color using HSV color space, precisely the S and V components.

Hu et al. [18] proposes a competent polarimetric recovery approach to enhance image quality on the basis of histogram attenuation prior while keeping in mind the benefit of the polarisation filter that contains a precisely constructed histogram processing technique called “cut-tail histogram stretching. The performance of the restoration can be further enhanced

by this processing, which gets around the limitation of conventional histogram-based techniques. The use of physics-based dichromatic modelling (PDM) in combination with a method based on histogram-equalization (HE) approximation was also proposed [19]. Images that have been degraded by nature, including such underwater images, can be restored using the PDM, which explains the image formation process. However, it cannot guarantee that reconstructed image has better contrast. To reconstruct color irregularities and enhancement underwater photographs via context optimisation, this method suggests for approximating the traditional HE on the basis of PDM. Address the issues of color cast as well as poor contrast, a method to enhance underwater images related to colour correction and three-interval histograms stretching is presented [20]. Initially, a sub-interval linear transformation related color improvement technique is intended to correct color. In the meantime, the contrast is improved utilising three adaptive sub-histogram equalisation algorithms, and the images produced by the aforementioned techniques are then blended using multi-scale fusion. A Bayesian retinex method is introduced by Zhuang et al. [6] utilising multi-order gradient reflectance and illumination priors. An efficient color correction technique is used for removal of color casts and restore naturalness. An underwater enhancing procedure on the basis of retinex inspired color correction and information preservation fusion method is presented [21] to address various issues in underwater images. To start, this technique uses a Retinex inspired color correction method modelled for getting rid of color casts caused via scattering of lights. Further, blend three images obtained from color corrected local contrast improved version, global contrast improved and detail version of underwater images.

A method based on Retinex is introduced by Hassan et al. [22]. The underwater image is first enhanced utilising CLAHE that reduces noise while enhancing brightness of image components at the expense of blurring the visual details. This strategy further performs Retinex based enhancement to recover the distorted colours. The novel enhancement was recently presented [23]. The lighting components are obtained utilising multiscale retinex approach. By linear quantisation, mean as well as mean square errors are introduced, and recovery of color factors are utilised for adjusting three channels for color improvement. Next, image noise is removed and the edge information are retained by considering image as anisotropic thermal diffusion in whole directions. Multi-featured prior fusion (MFPF) approach is proposed for improving perceptual quality of images [7]. Thus, the

final obtained underwater images will have better visual quality thanks to complementary multi-features. This method proposed a self-adaptive standard deviation based on color improvement technique that realizes color offset improvement on the basis of dominant color of an image. The brightness and structural details of the dark region were improved and are used to generate group of synthetic exposure maps arrangements from the low contrast images. For enhancing image quality, Wu et al.[24] developed a multiscale fusion GAN. This technique uses four convolutional branches to polish the information of three prior inputs as well as encode a source input, and blend the prior features utilising multiscale fusion networks that have been introduced, and then employs a channel attention decoder to produce better results. To boost the visual presentation of images, a two-stage approach on the basis of color correction and image fusion by combination of deep learning and traditional image enhancing method was proposed [25]. First, a method for adaptive color compensation is traduced to replace the strongly attenuated channels that were lost. Color restoration is also used to compute the illumination of color casts triggered through selective attenuation light. Due to the fact that underwater

photograph still has scattering and blurring after color restoration, a powerful technique on the basis of DIWF and GAN is developed that will additionally improve edge and contrast information. An effective and reliable enhancement of underwater images method called MLLE is developed by Zhang et al. [26]. This technique starts by locally adjusting the color of source image and information. Mean as well as variance of local image block are then computed using integral and squared maps that are used for adaptively control image contrast. Recently, Ucolor, a network for enhancement of underwater photograph was introduced [27]. In practice, this method first uses a multicolour space encoder network by fusing information of different color spaces into a single structure that enhances a variety of feature representations. Combined with the attenuation process, the maximum discriminative features that are obtained from many color-space that are adaptively incorporated and highlighted. In order to enhancing underwater images, Zhuang et al. [28] introduces a hyper Laplacian reflectance priors influenced retinex variational model. In precise, first and the second order reflectance gradient $l_{1/2}$ -norm penalty is used to define the hyper-Laplacian.

Table 1. Summary of some of the underwater image enhancing models.

Ref.	Year	Method	Approach used	Performance metrics	Advantage
Zhuang et al. [6]	2021	Bayesian retinex algorithm	The multioorder gradient priors is used to create a maximum a posteriori (MAP) formulation that applies 1 st order and 2 nd order gradient priors to both reflectance and illumination in order to better capture the finer scale and full structures.	UIQM, UICM, UIConM, UISM, CCF, UCIQE, NIQMC and Entropy	The extensive investigations demonstrate the successful results in case of colour accuracy, parameter evaluation, and algorithm convergence
Liu et al. [8]	2019	Deep learning	The CycleGAN are presented to generate synthetic underwater photographs as training dataset for CNN models and underwater RasNet model which is the residual learning model is applied for enhancement tasks.	PSNR, SSIM, UICM, UISM, UIConM and UIQM	The visual effects of underwater images are greatly enhanced, which is beneficial for the execution of vision related underwater tasks.
Yang et al. [9]	2021	Deep convolutional neural networks (CNNs)	An encoder decoder method with numerous AAF schemes composed of lightweight adaptive feature fusion network (LAFFNet). AAF generates multi-scale feature maps by combining branches with various kernel sizes. Furthermore, these	PSNR, SSIM, UIQM	In this model, AAF schemes were able to extract multiscale features and combine them by channel attention instead of down- and up-sampling. In addition, it designs the lightweight model quicker

			feature maps are adaptively combined via channel attention.		than other cutting-edge models by reducing the channel of convolutions.
Hu et al. [18]	2021	Histogram attenuation prior	It combines the polarimetric recovery model with a specific kind of local histogram processing. By employing a polarisation filter to create a cross-linear image, it further improves the contrast.	BRISQUE, EME, NIQE, Entropy	An efficient local histogram-based polarimetric recovery technique that can greatly improve image contrast and partially correct colour distortion.
Zhuang et al. [28]	2022	Retinex variational model	The retinex variational model was influenced by hyper-Laplacian reflectance priors. In particular, the 1 st order and 2 nd order reflectance gradients' $l_{1/2}$ -norm penalties are used to generate the hyper Laplacian reflectance priors.	UCIQE, PCQI, UIQM and Entropy	This technique is more effective at penalising multi-order gradients in terms of reflectance that enhances edges and details as well as restores the true colours. l_2 -norm is also useful for enforcing linear smoothness on the illumination as well as spatial smoothness.
Jiang et al. [34]	2022	Adversarial fusion network	Using manually created multi-scale dense enhanced muddy restoration and deep aesthetic colour correction schemes, we create a target oriented perceptual adversarial fusion network.	UCIQE, UIQM, UISM, UICM, UICoM, PSNR, SSIM, PCQI	The restoration of photographs with vibrant appearances and substantial contents works better with this technique.

reflectance priors. Such priors make use of complete-comprehensive and sparsity-promoting reflectance to improve both salient structures and tiny information, and restore the authenticity of real color. Furthermore, it is observed that $l_{1/2}$ -norm tends to work well for calculating illumination accurately.

The deep learning has recently demonstrated to perform exceptional in different computer vision works such as image segmentation [29], image defogging [30], super-resolutions [31], [32], and salient object detection [33]. Furthermore, deep learning-based methods are steadily used to enhancing underwater images [34], [35]. The strategy developed by Liu et al. [8] uses a deep residual structure. First, convolution neural network (CNN) models are trained using synthetic underwater images produced by CycleGAN. The Underwater Resnet model, a residual learning model for improving enhancing tasks is introduced along with a VDSR. Recently use of a LAFFNet was for enhancing underwater images [9]. An encoder-decoder design along with many AAF schemes constitute this model. The AAF generates multi-scale

feature maps by combining branches with various kernel sizes. Moreover, these feature maps are adaptively combined using channel attention. To accomplish both perceptibility and task-oriented enhancement, a new enhancement model was proposed [10]. In order to put it more precisely, it reduces the need of paired data when using an un-supervised method and maintains highly significant details by combining with “twin inverse mapping. Besides, it uses contrastive cues during training phase to give reconstructed image more realistic appearance. The novel enhancing model was presented by Lin et al. [35] and can asymptotically improve underwater image quality. The generator specifically includes an advanced enhancement system and two independent networks. The base image as well as several other parameter maps are needed for progressive enhancement are produced by dual-branch framework, respectively. It is suggested that underwater image quality be iteratively increased using the progressive enhancement algorithm. According to Huang et al. [36], an AGA could dynamically choose visually

complementary channels on the basis of dependencies thereby requiring fewer additional attention parameters. The TOPEL was recently proposed [34]. This method precisely considers the turbidity and chromatism factors that contribute to underwater image degradation. The process first makes a deep aesthetic render scheme in order to fortify perceptual contrast and implement color correction, respectively.

The DCAM is then used which is followed by a guided adaptive fusion of latent features that incorporates manifold information and showcase appropriate perceptibility. In the reconstruction, a global local adversarial system is incorporated to close the gap across synthetic and real-world datasets. Summary of some of the methods has been tabulated in Table 1.

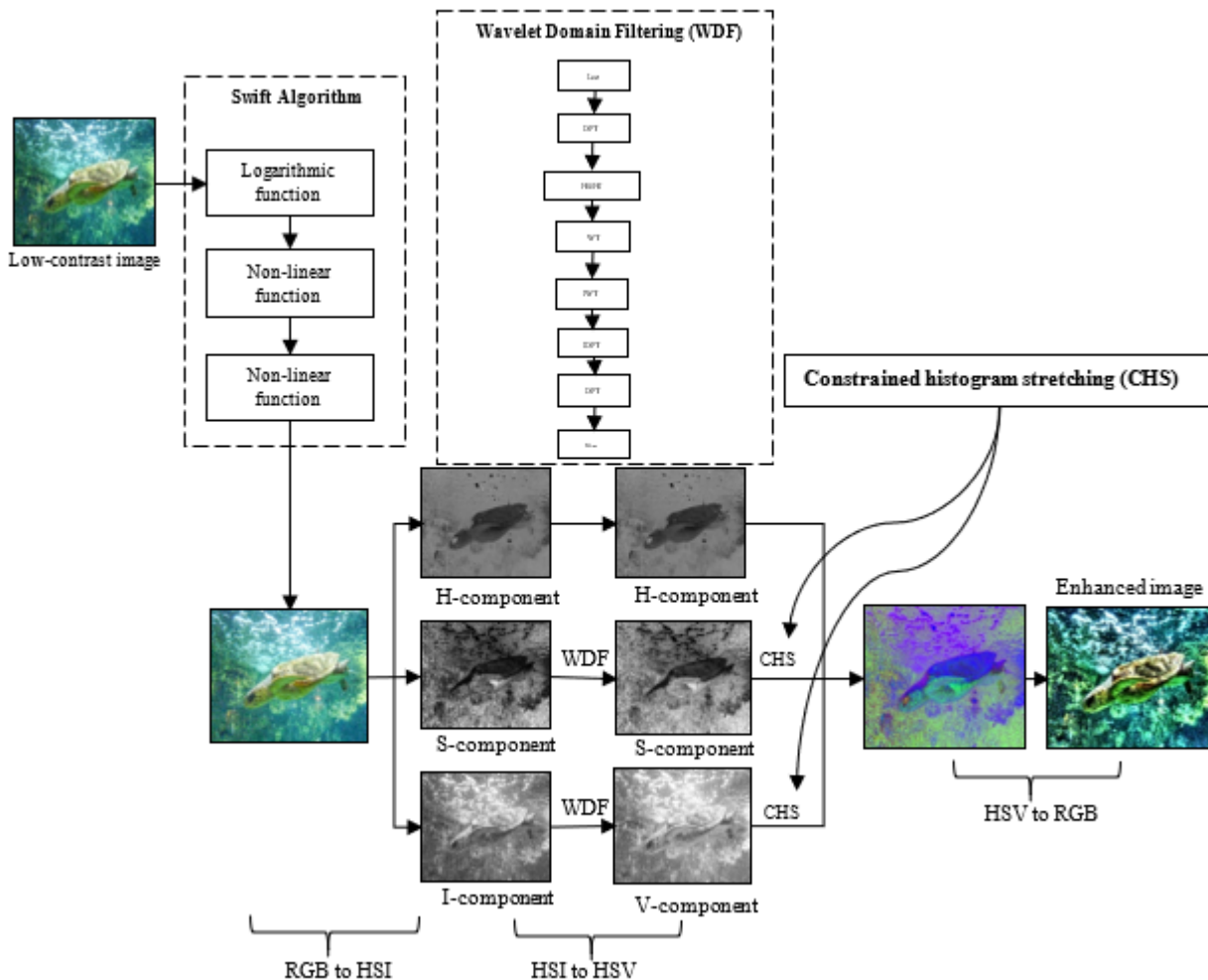


Fig.2. Methodological flowchart of the proposed algorithm

3. Methodology

This section summarises overall stages of the proposed algorithm. The schematic flowchart for our method is shown in Fig. 2. A swift algorithm for enhancing contrast in images is introduced in the first stage. It consists of three distinct steps: (a) a preliminary preprocessing step for reducing the excessive pixel values, (b) a subsequent processing step for modifying brightness and contrast, (c) a concluding postprocessing stage to rearrange pixels to their natural dynamic range. In addition, as illustrated in Sections 2.1.1 and 2.1.2, a conversion across RGB color models and the HSV/HIS color model is provided. Then, in Section 2.2, the enhancement model for underwater

colour model utilising the hue preservation technique is described.

3.1 Swift algorithm

This algorithm attenuates the immoderate pixel values and modify the contrast of both images[37]. At preprocessing phase, it uses a non-complex logarithmic function to obtain a suited intensity equalization and remove immoderate pixel values. If not managed properly such immoderate levels can result in excessive whiteness. The following is how the logarithmic operation is computed [38] as

$$u_{(x,y)} = \log(1 + \bar{G}_{(x,y)}) \quad (1)$$

where $\bar{G}_{(x,y)}$ represents an above filtered image having intensity in the range $[0, -1]$, $u_{(x,y)}$ represents an output image from preprocessing stage, and (x, y) indicate the special coordinates. The adjustment function is determined and will be utilized later in novel constructed magnitude modification function. The initial adjustment parameter ζ , that is a rectified sample standard deviation of an image $u_{(x,y)}$ is the technique which can be used to compute an extant of variation and distribution in the set of pixel scores. In computer vision, ζ is a sensible to contrast attributes where image having poor contrast will carry low ζ scores than image having high contrast. The adjustment factor ζ is determined by [39] as

$$\zeta = \sqrt{\frac{1}{n-1} \sum_{i=1}^n (u_i - \bar{u})^2} \quad (2)$$

$$\bar{u} = \frac{1}{n} \sum_{i=1}^n u^i \quad (3)$$

where u^i represents vector representation of an image $u_{(x,y)}$ and \bar{u} represent average of u^i . Further, n represents number of components at maximum size in u_i . Therefore, the second adjustment function η is computed utilizing following equations.

$$\eta = \frac{(u_{(x,y)})^\lambda}{\lambda!} \quad (4)$$

where λ denotes a tweaking function that is set as default ($\lambda = 3$). An image $u_{(x,y)}$ is next subjected to the actual processing step which adjust the brightness and contrast. This process entails the implementation of a new nonlinear function relating to mathematical, statistical, and spatial details designed experimentally. The following is how the nonlinear function is determined as

$$f_{(x,y)} = \exp\left(\frac{\tan(u_{(x,y)} - \zeta)}{\exp(u_{(x,y)} - \eta)}\right)^r \quad (5)$$

where \tan represents a tangent in radius of each image pixel $u_{(x,y)}$ and $f_{(x,y)}$ represents a photograph with improved tonality. Where r denotes an adjustment factor which governs a level of enhancement and must

fulfil $r > 0$, where a low r value resulting in brighter contrast enhancement results and a high r value resulting in less-bright contrast enhancement results. Above equation has the substantial impact on image tonality enhancement. Thus, using the tangent in radians and elementwise exponential parameters helps to generate two dissimilar curve transformation for filtered images. When these two parameters are utilized with adjustment factors ζ and η , they prefer for enhancing brightness and generate perceptible tone shift in some situations. The values and experimental function are decreased by two separate adjustment factors ζ and η , and to overcome such effects. Both functions could provide an enhanced curvilinear transformation for the utilized functions. The parameter ζ is the common measure which can be utilized in numerous real-world applications however η are obtains experimentally. One last hurdle that should be deal with is a photograph contrast $f_{(x,y)}$ is restricted for the specific dynamic range. Therefore, it must be regularized to provide suited quality performance. Thus, as a last postprocessing step, a regularization function is used for redistribution of image pixels to their native dynamic range. The regularisation operator that was used could be determined as in [40].

3.2 Colour models

The RGB model which is most widely used and is present in practically each computer system, TV and video is described by three chromaticity of green, red and blue additive primaries. A unit cube is typically used to display the RGB model, which is sensitive to variations in lighting intensity. We therefore look for other illumination-invariant color model. The HSV/HIS model is a nonlinear version of RGB colour model and it defines colour highly accurate for human interpretation than the RGB model does [41]. Three components make up the HSI/HSV colour model: HSI/V. Both colour models are broadly utilised in the fields of computer vision since each one's three components may be handled independently and separately.

3.2.1 RGB-HIS conversion: The results range from 0-360 for H and from 0-1 for S and I when RGB variables have values between 0 and 255. The HSI formulas are [42]:

$$H = \begin{cases} \theta & \text{if } B \leq G \\ 360 - \theta & \text{if } B > G \end{cases}$$

with θ

$$= \cos^{-1} \frac{\{(1/2)[R - G] + (R - B)\}}{[(R - G)^2 + (R - G)(R - B)]^{1/2}}$$

$$S = 1 - \frac{3[\min(R, G, B)]}{(R + G + B)} \quad (7)$$

$$I = \frac{1}{2}(R + G + B) \quad (8)$$

3.2.2 RGB–HSV conversion: According to Travis [43], the conversion of RGB to HSV is based on the normalised RGB values:

$$H = \begin{cases} 5 + B' & \text{if } R = \text{MAX and } G = \text{MIN} \\ 1 - G' & \text{if } R = \text{MAX and } G \neq \text{MIN} \\ 1 + R' & \text{if } G = \text{MAX and } B = \text{MIN} \\ 3 - B' & \text{if } G = \text{MAX and } B \neq \text{MIN} \\ 5 + G' & \text{if } R = \text{MAX} \\ 5 - R' & \text{otherwise} \end{cases} \times 60 \quad (9)$$

$$S = 1 - \frac{\text{MIN}}{\text{MAX}} \quad (10)$$

$$V = \text{MAX}, \quad (11)$$

$$\text{MAX} = \max(R, G, B) \quad \text{MIN} = \min(R, G, B)$$

$$R' = \frac{\text{MAX}-R}{\text{MAX}-\text{MIN}} \quad G' = \frac{\text{MAX}-G}{\text{MAX}-\text{MIN}} \quad B' = \frac{\text{MAX}-B}{\text{MAX}-\text{MIN}}$$

3.3 Enhancement algorithms

This strategy uses a two-step method. Prior to using WDF technique on the saturation coefficient of S and intensity coefficient I, an image is first transformed from RGB model to HIS model while preserving hue coefficient H. The component H is then continuously kept during the conversion to HSV color model and the CHS scheme is utilised to stretch S and V components. As previously said, the proposed method contains various stages. Fig. 2 depicts the processing flowchart for our method.

3.3.1 WDF in HIS color model

The conventional HF [44] is generalised in image processing technique that combines grey-level transformation and frequency filtering. It could be utilised in reducing effects of uneven lighting and improve image information. Here, the WDF method that could be reduce noise that is amplified by enhancement process. A photograph is made up of frequency component $i(x, y)$ as well as reflectance component $r(x, y)$ of lightning when the image formation is taken into account, as well as the characteristics of light. The illustration in provided by

$$\begin{aligned} f(x, y) &= i(x, y) \\ &\times r(x, y) \end{aligned} \quad (12)$$

The following six steps composed the WD filter method implementation:

Step 1: Using the logarithm of the image to separate the components of illumination and reflectance:

$$\begin{aligned} g(x, y) &= \ln(f(x, y)) \\ &= \ln(i(x, y)) \times r(x, y) \\ &= \ln(i(x, y)) + \ln(r(x, y)) \end{aligned} \quad (13)$$

Step 2: After taking a logarithm, calculate the fourier transform of an image;

$$\begin{aligned} G(\omega_x, \omega_y) &= I(\omega_x, \omega_y) \\ &+ R(\omega_x, \omega_y) \end{aligned} \quad (14)$$

Step 3: Filtering in the frequency domain using the homomorphic filter $H(u, v)$.

$$\begin{aligned} S(\omega_x, \omega_y) &= H(\omega_x, \omega_y) \times I(\omega_x, \omega_y) \\ &+ H(\omega_x, \omega_y) \times R(\omega_x, \omega_y) \end{aligned} \quad (15)$$

$$\text{where } H(\omega_x, \omega_y) = \left(1 - \exp\left(-\left(\frac{\omega_x^2 + \omega_y^2}{2\delta_\omega^2}\right)\right)\right) \times (r_H - r_L) + r_L,$$

where the cut-off frequency is controlled by a factor δ_ω , and the maximal and coefficient values are $r_H = 2.5$ and $r_L = 0.5$. These parameters are chosen empirically.

Step 4: Multiscale soft thresholding for denoising in WD. Use the following thresholding formula to the wavelet coefficient at each level:

$$W'T_{i,j} = \begin{cases} W'T_{i,j} - T_{i,j} & W'T_{i,j} > T_{i,j} \\ W'T_{i,j} + T_{i,j} & W'T_{i,j} < -T_{i,j} \\ 0 & |W'T_{i,j}| < T_{i,j} \end{cases} \quad (16)$$

$$\text{where } W'T_{i,j} = \lambda \cdot WT_{i,j}$$

where $T_{i,j}$ represent threshold value, i is the wavelet scale coefficient and λ is the enhancing component where $j = 1, 2, 3, (HH, HL, LH)$.

Step 5: Estimation of an inverse wavelet transform as well as reconstruction of wavelet component.

Step 6: An inverse fourier transform are computed to restore the spatial domain and the exponent is than used to get the filtered image.

When the WDF method is applied to the degraded image, the contrast can be improved, non-uniform lighting issues can be resolved, and accidentally amplified noise can be suppressed, however colour imbalance could result. Similar to the HSI colour model, the elements S and I

provide a larger variety of colours while coefficient H determines color of an image. Only S and I are used in this instance of the WDF method while coefficient H is preserved.

3.3.2 CHS in HSV color model

It is an easy and simple procedure to enhance images which differs from histogram equalisation, which is more complex. The pixel values which aim to improve contrast in the image are scaled linearly as a result. To do this, a desired range of values is covered through stretching a range of I values. The formula below is used to scale each pixel individually:

$$\begin{aligned} P_{out} & \\ &= (P_{in} - c) \frac{(b - a)}{(d - c)} \\ &+ a \end{aligned} \quad (17)$$

where P_{out} represents normalised pixel value and P_{in} represents pixel value, where a and b upper and lower value limits, c and d represent the lowest and higher pixel values presently contain in the images, respectively. Same as WDF processing approach, component H is preserved maintained continuously in this case as well to guarantee colour fidelity. Additionally, stretching the S and I values of HSV color model utilising an above-mentioned transform function on S and V components.

4. Experimental Results and Discussion

Several existing methods are utilised to validate the performance of the proposed method, namely robust back scattered light estimation with polarisation (RBLE-P) [13], twin adversarial contrastive learning (TACL) [10], Bayesian retinex underwater image enhancement (BRUIE) [6], deep residual framework (DRF) [8] and LaFFNet [9]. The enhancement performance of each algorithm is assessed both visually and quantitatively. We run the source code with the recommended parameter settings provided by the corresponding authors for obtaining best possible results for both quantitative and qualitative assessments. In terms of quantitative analysis, it is primarily computed in terms of SSIM, PSNR [1] [45], UIQM [1] and PCQI [1]. An enhanced image with higher visibility is signified by an entropy value that is high. The high PCQI value signifies an enhancement image with higher contrast. The high UIQM value signifies that an enhanced image has improved luminance, saturation, chroma balance. In the experiment, we analysed our method using a standard underwater dataset made available by Li et al. [46]. The dataset contains 893 underwater images that were found online. As can be seen in Fig. 3-7, we selected a number of underwater degraded photographs that were

taken in various challenge scenarios (low-light, bluish, turbid, and with artificial lightning) for comparison.

4.1. Parameters Settings

In case of existing LDCT image denoising techniques (i.e., RBLE-P, TACL, BRUIE, DRF and LaFFNet), parameters are set as instructed by the authors of the respective articles. In terms of proposed algorithm, the parameters. In terms of proposed algorithm, the λ indicates a tweaking parameter which by default is considered as 3. The maximal and the minimal component values represented by r_H and r_L is 2.5 and 0.5. Further, δ_ω indicates a factor that controls the cutoff frequency. The simulations is conducted in MATLAB R2019b on the 64-bit Windows 10 PC with an Intel (R) Core (TM) i9-9900k CPU running at 3.6 GHz and 16 GB of RAM.

4.2. Qualitative evaluation

This section evaluates the performance of proposed method visually along with different image enhancement and restoration techniques such as DRF, BRUIE, LaFFNet, RBLE-P, and TACL method. Two strategies are typically used to assess the results of underwater photographs; both qualitative and quantitative assessment. In terms of comparison, as seen in Fig. 3-7, we selected a number of underwater degraded photographs taken in various challenge scenarios. The underwater images in Fig. 3 show a variety of greenish conditions, which appear to be the norm in coastal waters. It is noticeable that the proposed method, the TACL technique and the BRUIE method all greatly increase perceptibility. However only the proposed approach and TACL can bring back more vibrant colour. As observed in 3rd column of Fig. 3(b), the BRUIE approach, in contrast, has the issue of injecting excessive red colour into the restored output. The natural green tones in the image are also aggravated by the DRF technique. Both the LaFFNet and RBLE-P techniques fall short in terms of revealing scene details, and neither one is able to adjust the image's overall tones. The blueish image makes it difficult and challenging for most underwater dehazing techniques to work. This situation prevents the green channel from maintaining its intensity which prevents it from offering enough valuable data for photograph improvement or restoration. As seen in Fig.4, the methods of DRF, BRUIE, LaFFNet, and RBLE-P have little impact on resolving this issue. Although it contributes to colour correction, TACL appears to be less robust as observed in 2nd to final column of Fig.4. Fortunately, the obtained findings of our strategy successfully address this problem by revealing more information and achieving an acceptable colour performance. The unfavourable consequences of dispersion become more obvious in a setting with murky waters. In this situation, it can give the contrasted approaches a good opportunity to assess how well they

perform when dehazing. Fig. 5 displays the matching retrieved results produced from three typical underwater images shot in murky conditions. In reality, the conventional method contributes to haze removal; nevertheless, variations of this algorithm like BRUIE and RBLE-P can also significantly reduce the appearance of haze. But both of these methods will reduce overall brightness of the images by producing unpleasant visual effects. Similar to the BRUIE method, the results of TACL algorithm are prone to whitening the intended situation. Additionally, their inability to discern certain features is hampered by their lack of sharpness. The reconstructed outputs produced by our technique are

better to these algorithms in case of dehazing notably for maintaining colour accuracy. In addition to colour cast and dispersion, restoration of lighting is another problem that needs to be resolved for the low-light situation. As seen in Fig. 6, while the RBLE-P approach definitely over enhances the red and green channel and as a result introduces some additional colour deviation, the DRF method reduces image brightness. The results of the BRUIE, LaFFNet, and TACL based approaches can marginally increase visibility, but they are still lacking. On the other hand, the method we proposed is more effective at colour restoration and illumination recovery, and it

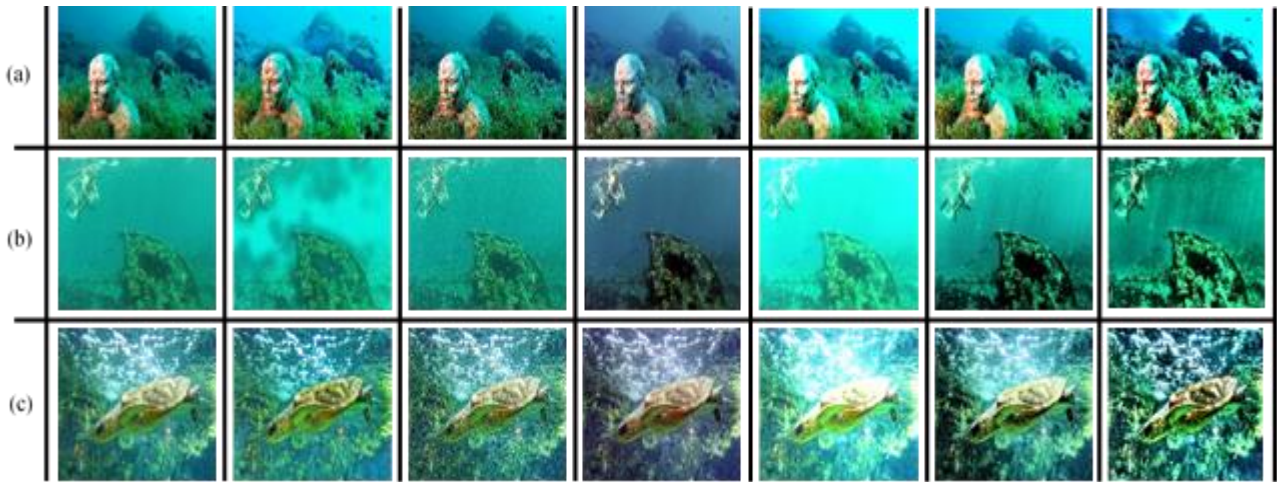


Fig.3. Comparative analysis of underwater greenish scene. From left to right; original image and the results generated by DRF, BRUIE, LaFFNet, RBLE-P, TACL and ours, respectively.



Fig.4. Comparative analysis of underwater bluish scene. From left to right; original image and the results generated by DRF, BRUIE, LaFFNet, RBLE-P, TACL and ours, respectively.

also reveals more details that were before buried in darker regions. The underwater photography with artificial lighting is a unique but not uncommon situation. The utilisation of artificial lighting is required in some water locations where natural light is obstructed or diminished. The capacity to isolate its influence and appropriately reconstruct or enhance the photograph is the main criterion to evaluate the performance of the underwater

dehazing algorithms because of several light attenuation rates in the artificial lighting regions. The experimental results of DRF and LaFFNet approach which are shown in Fig. 7 are not as good as anticipated because they initially do not take this circumstance into consideration. Although the BRUIE method reasonably avoided influence of this regions, the overall response of image is not immediately apparent. In contrast to BRUIE, the

RBLE-P algorithm is unable to prevent the issue of over enhancing caused by the uneven illumination. However, the TACL method and our technique can discreetly brighten the images and improve contrast in the darker areas. It has been discovered that our technique can produce more precise features and a sharper edge contour

when compared to the TACL method. We provide several additional examples with higher textural structure and histogram in Fig. 8 to further demonstrate this superiority. There is a clear difference between the TACL and our approach. We also include histogram of



Fig.5. Comparative analysis of underwater turbid scene. From left to right; original image and the results generated by DRF, BRUIE, LaFFNet, RBLE-P, TACL and ours, respectively.

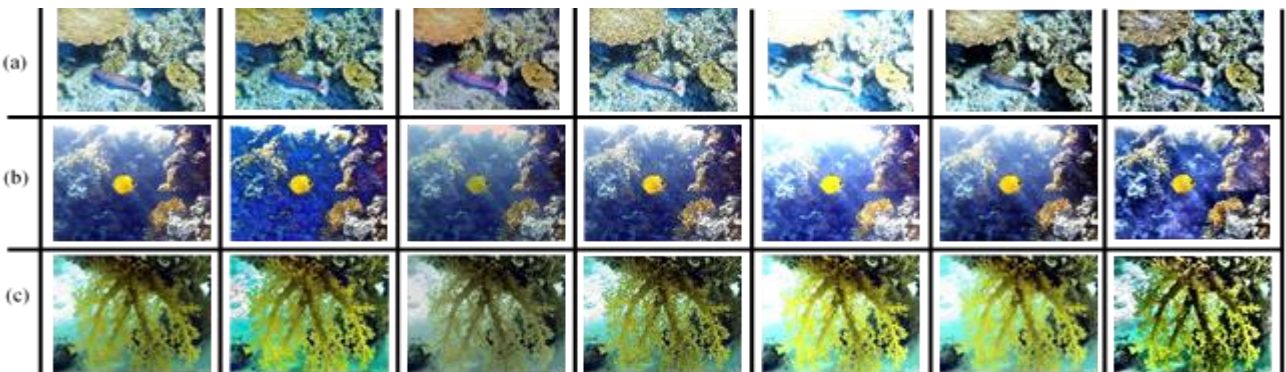


Fig.6. Comparative analysis of underwater low light scene. From left to right; original image and the results generated by DRF, BRUIE, LaFFNet, RBLE-P, TACL and ours, respectively.



Fig.7. Comparative analysis of underwater artificial lighting scene. From left to right; original image and the results generated by DRF, BRUIE, LaFFNet, RBLE-P, TACL and ours, respectively.

RGB colours of some original and restored images in Fig. 8. Clearly, the proposed technique surpasses the TACL method in case of edge performance and discloses more information

4.3. Quantitative evaluation

We use a number of objective indicators including PSNR, SSIM, UIQM, and PCQI, which are frequently used to

analyse performance for the underwater image enhancement quantitative assessment. The PSNR calculates the intensity difference across the ground truth photograph and the enhanced photograph. The SSIM metric measures how similar two images are to one another. On the basis of structural data, SSIM offers accuracy. The UIQM and PCQI measures are specifically

made for evaluating underwater images, whereas SSIM and PSNR are general-purpose metrics for evaluating image contrast. While the PCQI measure us utilised to assess the visual distortion of a photograph by

decomposing an image mean intensity, signal intensity and signal structural components by adaptive representation of local patches, the UIQM

Table 2. Quantitative analysis of the reconstructed images presented in Figs. 3-7 using PSNR, SSIM, PCQI and UIQM measures. The bold values indicate the best scores.

Assessments for underwater images with greenish scene (Fig.3)																								
DRF				BRUIE				LaFFNet				RBLE-P				TACL				Proposed				
	P S N R	S SI M	U IQ M	P C Q I	P S N R	S SI M	U IQ M	P C Q I	PS N R	S SI M	U IQ M	P C Q I	P S N R	S SI M	U IQ M	P C Q I	P S N R	S SI M	U IQ M	P C Q I	P S N R	S SI M	U IQ M	P C Q I
(a)	25.62	0.84	1.23	0.95	28.67	0.86	1.27	0.98	29.11	0.87	1.34	1.07	30.98	0.88	1.37	1.10	31.66	0.90	1.39	1.13	33.72	0.92	1.45	1.16
(b)	24.88	0.82	1.04	1.03	26.18	0.85	1.10	1.08	28.19	0.89	1.17	1.15	29.19	0.90	1.21	1.20	30.66	0.91	1.35	1.24	32.77	0.93	1.37	1.27
(c)	26.89	0.85	1.02	0.99	29.56	0.87	1.10	1.04	31.89	0.88	1.15	1.13	32.99	0.91	1.20	1.18	33.22	0.93	1.34	1.21	34.67	0.94	1.36	1.23
Assessments for underwater images with blueish scene (Fig.4)																								
DRF				BRUIE				LaFFNet				RBLE-P				TACL				Proposed				
	P S N R	S SI M	U IQ M	P C Q I	P S N R	S SI M	U IQ M	P C Q I	PS N R	S SI M	U IQ M	P C Q I	P S N R	S SI M	U IQ M	P C Q I	P S N R	S SI M	U IQ M	P C Q I	P S N R	S SI M	U IQ M	P C Q I
(a)	24.67	0.83	1.06	0.95	26.88	0.85	1.11	0.97	28.99	0.86	1.16	1.01	30.24	0.88	1.23	1.05	31.87	0.90	1.26	1.09	32.18	0.92	1.32	1.13
(b)	25.63	0.84	1.02	0.96	27.27	0.87	1.05	0.98	29.12	0.88	1.08	1.04	30.56	0.91	1.34	1.11	32.16	0.92	1.37	1.15	33.89	0.94	1.43	1.21
(c)	23.99	0.82	0.94	0.93	25.77	0.86	0.99	0.96	27.78	0.87	0.99	0.99	29.11	0.90	1.28	1.02	30.77	0.92	1.31	1.06	32.19	0.95	1.34	1.10
Assessments for underwater images with turbid scene (Fig.5)																								
DRF				BRUIE				LaFFNet				RBLE-P				TACL				Proposed				
	P S N R	S SI M	U IQ M	P C Q I	P S N R	S SI M	U IQ M	P C Q I	PS N R	S SI M	U IQ M	P C Q I	P S N R	S SI M	U IQ M	P C Q I	P S N R	S SI M	U IQ M	P C Q I	P S N R	S SI M	U IQ M	P C Q I
(a)	25.89	0.85	1.01	0.87	27.37	0.87	1.05	0.98	29.17	0.89	1.11	0.91	32.77	0.91	1.15	0.94	34.62	0.93	1.19	0.97	36.27	0.95	1.23	0.98

(b)	26.15	0.83	1.02	0.85	28.14	0.85	1.06	0.90	29.15	0.87	1.13	0.92	31.56	0.89	1.17	0.96	33.11	0.91	1.22	0.99	34.26	0.93	1.27	1.03
(c)	24.89	0.84	0.96	0.86	26.19	0.86	0.98	0.95	28.92	0.88	1.02	0.98	30.13	0.90	1.05	1.01	32.67	0.92	1.07	1.06	33.29	0.94	1.13	1.12

Assessments for underwater images with low-light scene (Fig.6)

	DRF				BRUIE				LaFFNet				RBLE-P				TACL				Proposed			
	P S N R	S S I M	U I Q M	P C Q I	P S N R	S S I M	U I Q M	P C Q I	PS N R	S S I M	U I Q M	P C Q I	P S N R	S S I M	U I Q M	P C Q I	P S N R	S S I M	U I Q M	P C Q I	P S N R	S S I M	U I Q M	P C Q I
(a)	23.78	0.82	1.02	0.90	25.84	0.84	1.06	0.93	27.88	0.86	1.10	0.95	29.23	0.88	1.14	0.98	31.88	0.90	1.18	1.01	33.26	0.93	1.23	1.05
(b)	22.67	0.81	1.08	0.86	24.56	0.83	1.12	0.89	26.89	0.84	1.16	0.91	28.62	0.87	1.21	0.93	30.89	0.89	1.24	0.95	32.18	0.92	1.27	0.99
(c)	22.16	0.80	0.99	0.95	23.92	0.82	1.03	0.98	26.16	0.83	1.08	1.00	27.99	0.85	1.13	1.04	29.13	0.88	1.17	1.08	31.89	0.91	1.22	1.12

Assessments for underwater images with artificial lighting scene (Fig.7)

	DRF				BRUIE				LaFFNet				RBLE-P				TACL				Proposed			
	P S N R	S S I M	U I Q M	P C Q I	P S N R	S S I M	U I Q M	P C Q I	PS N R	S S I M	U I Q M	P C Q I	P S N R	S S I M	U I Q M	P C Q I	P S N R	S S I M	U I Q M	P C Q I	P S N R	S S I M	U I Q M	P C Q I
(a)	24.67	0.81	0.85	0.94	26.14	0.83	0.87	0.97	27.87	0.86	0.89	1.00	29.66	0.89	0.92	1.05	31.88	0.91	0.96	1.09	33.27	0.93	0.99	1.14
(b)	26.78	0.84	0.93	0.86	28.56	0.86	0.96	0.89	30.15	0.88	0.99	0.90	31.52	0.90	1.04	0.92	33.86	0.93	1.08	0.94	35.87	0.95	1.11	0.98
(c)	25.89	0.80	0.92	0.88	27.17	0.83	0.95	0.90	28.93	0.86	0.98	0.92	30.98	0.88	1.03	0.95	32.87	0.91	1.07	0.98	34.27	0.94	1.12	1.03

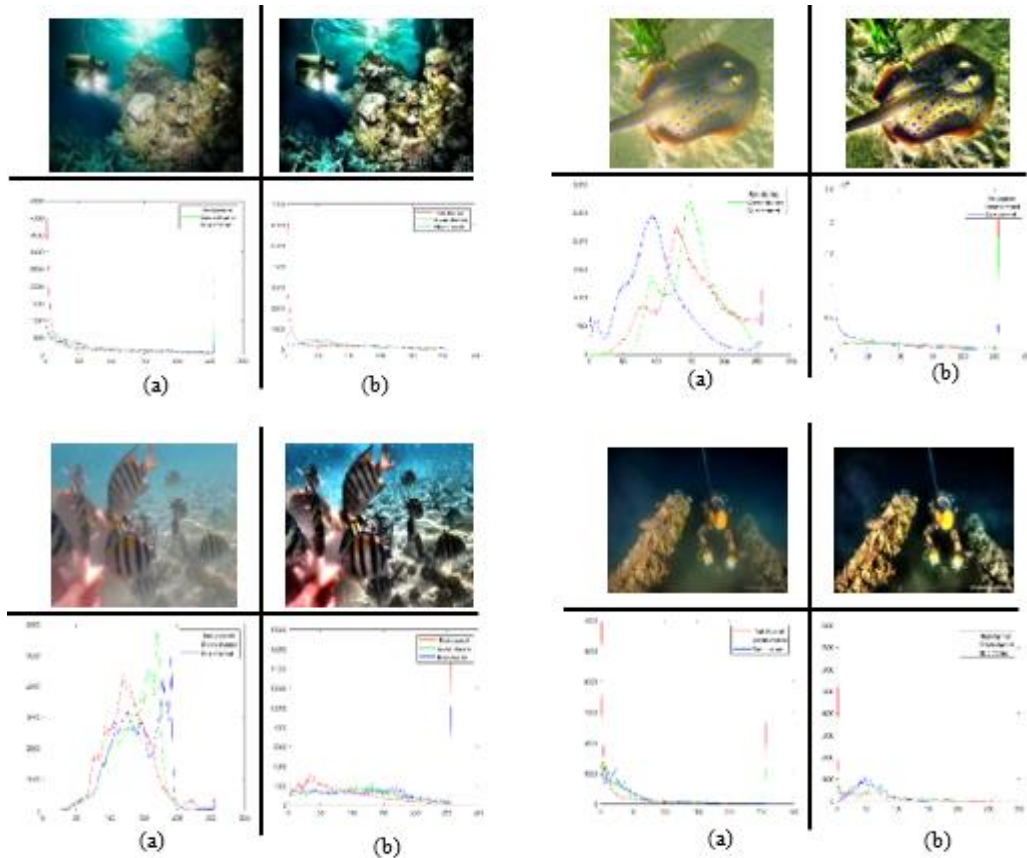


Fig.8. Comparisons of histograms distributions of R, G, B channels; (a) Original images and (b) the results of proposed method

measures image performance through a linear combination of colourfulness. Table 2 displays the quantitative evaluation findings from Figs. 3–7 produced by the five comparative approaches and the proposed methodology. The higher values show the better performance for all metrics. Regarding the greenish image and the image taken under artificial illumination, it could be observed that proposed technique achieves nearly the better values across all parameters due to its excellent effectiveness in boosting contrast and reviving bright colour. Since DRF, BRUIE, and LaFFNet technique scores are typically close to 1, they have little impact on contrast for blueish images. Although TACL performs better in terms of PCQI and UIQM, its limited resilience and colour accuracy render it useless. The results that BRUIE and LaFFNet techniques obtained in the murky water and dimly lit scenario have a lot of dark patches. Additionally, their irregular high PCQI and UIQM readings are aberrant and at odds with the subjective perceptual assessment. In spite of this, the proposed technique still obtains ideal results in terms of PCQI and UIQM metrics when compared to other methods. It can be observed from the Table 2, the more PSNR and SSIM scores verify that the proposed method contributes on improving the contrast of the underwater photographs. Additionally, the PCQI and UIQM measures are generally above 0.8 and 1.5, respectively that further indicates

superiority of the proposed method in robustness for dehazing and colour correction. The average values of measures SSIM, PSNR, UIQM, and PCQI for the restored images produced by all of the methods that were compared. We may conclude from Table 2 that, in case of ideal values of the four metrics the proposed technique performs better than other comparative methodologies in terms of both visually and quantitative evaluation.

5. Conclusion and Future Work

In this research, we introduce a competent underwater image enhancing strategy based on swift algorithm and hue-preserving based method. There are three distinct steps in the swift algorithm: a preliminary preprocessing stage to reduce an excessive pixel value, a follow-up stage for modifying contrast and brightness and the final postprocessing stage for rearranging pixels to their native dynamic range. On the HIS and HSV color models, respectively, we used WDF and CHS techniques. The method is applied to a collection of underwater colour photographs and the experimental findings demonstrates how successfully the real-colour image dynamic range can be compressed while maintaining accurate colour reproduction and resolving non-uniform illumination. In terms of experimental findings, fifteen representative poor-quality photographs with several challenge scenes are chosen and compared to the other five popular

methods. The significant visual and quantitative results demonstrates that our strategy obtains better in case of improving visibility and colour interpretation. The great natural appearance and detail preservation are adequate to prove that proposed method is capable to eliminate noise generated by suspended particles. Additionally, the proposed framework can broaden its application in underwater computer visions and image processing such as target identification and image recognition in addition to contribution for better technique to address the problems of underwater image enhancement. We are constantly extending our framework to considers more elements that might damage underwater image quality. For instance, underwater images frequently experience motion blurring, yet this phenomenon is rarely deliberated in restoration and enhancement techniques. Additionally, one of our future research focuses will be on adapting our approach to handle video processing.

References

- [1] D. C. Lepcha, B. Goyal, A. Dogra, K. P. Sharma, and D. N. Gupta, "A deep journey into image enhancement: A survey of current and emerging trends," *Information Fusion*, vol. 93, pp. 36–76, May 2023, doi: 10.1016/J.INFFUS.2022.12.012.
- [2] J. Zhou, T. Yang, W. Chu, and W. Zhang, "Underwater image restoration via backscatter pixel prior and color compensation," *Eng Appl Artif Intell*, vol. 111, p. 104785, May 2022, doi: 10.1016/J.ENGAPPAI.2022.104785.
- [3] J. Zhou, Y. Wang, and W. Zhang, "Underwater Image Restoration via Information Distribution and Light Scattering Prior," *Computers and Electrical Engineering*, vol. 100, p. 107908, May 2022, doi: 10.1016/J.COMPELECENG.2022.107908.
- [4] J. Zhou et al., "Underwater image restoration via depth map and illumination estimation based on a single image," *Optics Express*, Vol. 29, Issue 19, pp. 29864–29886, vol. 29, no. 19, pp. 29864–29886, Sep. 2021, doi: 10.1364/OE.427839.
- [5] G. Ulutas and B. Ustubioglu, "Underwater image enhancement using contrast limited adaptive histogram equalization and layered difference representation," *Multimed Tools Appl*, vol. 80, no. 10, pp. 15067–15091, Apr. 2021, doi: 10.1007/S11042-020-10426-2/METRICS.
- [6] P. Zhuang, C. Li, and J. Wu, "Bayesian retinex underwater image enhancement," *Eng Appl Artif Intell*, vol. 101, p. 104171, May 2021, doi: 10.1016/J.ENGAPPAI.2021.104171.
- [7] J. Zhou, D. Zhang, and W. Zhang, "Underwater image enhancement method via multi-feature prior fusion," *Applied Intelligence*, vol. 52, no. 14, pp. 16435–16457, Nov. 2022, doi: 10.1007/S10489-022-03275-Z/METRICS.
- [8] P. Liu, G. Wang, H. Qi, C. Zhang, H. Zheng, and Z. Yu, "Underwater Image Enhancement with a Deep Residual Framework," *IEEE Access*, vol. 7, pp. 94614–94629, 2019, doi: 10.1109/ACCESS.2019.2928976.
- [9] H. H. Yang, K. C. Huang, and W. T. Chen, "LaFFNet: A Lightweight Adaptive Feature Fusion Network for Underwater Image Enhancement," *Proc IEEE Int Conf Robot Autom*, vol. 2021-May, pp. 685–692, 2021, doi: 10.1109/ICRA48506.2021.9561263.
- [10] R. Liu, Z. Jiang, S. Yang, and X. Fan, "Twin Adversarial Contrastive Learning for Underwater Image Enhancement and Beyond," *IEEE Transactions on Image Processing*, vol. 31, pp. 4922–4936, 2022, doi: 10.1109/TIP.2022.3190209.
- [11] G. Verma and M. Kumar, "Systematic review and analysis on underwater image enhancement methods, datasets, and evaluation metrics," <https://doi.org/10.1117/1.JEI.31.6.060901>, vol. 31, no. 6, p. 060901, Nov. 2022, doi: 10.1117/1.JEI.31.6.060901.
- [12] C. Brosseau, A. Alfalou, J. Hajjami, M. Elbouz, and K. O. Amer, "Enhancing underwater optical imaging by using a low-pass polarization filter," *Optics Express*, Vol. 27, Issue 2, pp. 621–643, vol. 27, no. 2, pp. 621–643, Jan. 2019, doi: 10.1364/OE.27.000621.
- [13] S. Chen, E. Chen, T. Ye, and C. Xue, "Robust back-scattered light estimation for underwater image enhancement with polarization," *Displays*, vol. 75, p. 102296, Dec. 2022, doi: 10.1016/J.DISPLA.2022.102296.
- [14] R. Sathya, M. Bharathi, and G. Dhivyasri, "Underwater image enhancement by dark channel prior," *2nd International Conference on Electronics and Communication Systems, ICECS 2015*, pp. 1119–1123, Jun. 2015, doi: 10.1109/ECS.2015.7124757.
- [15] J. Zhou et al., "Underwater image restoration via feature priors to estimate background light and optimized transmission map," *Optics Express*, Vol. 29, Issue 18, pp. 28228–28245, vol. 29, no. 18, pp. 28228–28245, Aug. 2021, doi: 10.1364/OE.432900.
- [16] P. K. Sharma, I. Bisht, and A. Sur, "Wavelength-based Attributed Deep Neural Network for Underwater Image Restoration," *ACM Transactions*

on Multimedia Computing, Communications and Applications, Jan. 2023, doi: 10.1145/3511021.

- [17] J. Zhou, Z. Liu, W. Zhang, D. Zhang, and W. Zhang, "Underwater image restoration based on secondary guided transmission map," *Multimed Tools Appl*, vol. 80, no. 5, pp. 7771–7788, Feb. 2021, doi: 10.1007/S11042-020-10049-7/METRICS.
- [18] H. Hu, P. Qi, X. Li, Z. Cheng, and T. Liu, "Underwater imaging enhancement based on a polarization filter and histogram attenuation prior," *J Phys D Appl Phys*, vol. 54, no. 17, p. 175102, Feb. 2021, doi: 10.1088/1361-6463/ABDC93.
- [19] Y. T. Peng, Y. R. Chen, Z. Chen, J. H. Wang, and S. C. Huang, "Underwater Image Enhancement Based on Histogram-Equalization Approximation Using Physics-Based Dichromatic Modeling," *Sensors* 2022, Vol. 22, Page 2168, vol. 22, no. 6, p. 2168, Mar. 2022, doi: 10.3390/S22062168.
- [20] J. Zhou, L. Pang, and W. Zhang, "Underwater image enhancement method based on color correction and three-interval histogram stretching," *Meas Sci Technol*, vol. 32, no. 11, p. 115405, Aug. 2021, doi: 10.1088/1361-6501/AC16EF.
- [21] W. Zhang, L. Dong, and W. Xu, "Retinex-inspired color correction and detail preserved fusion for underwater image enhancement," *Comput Electron Agric*, vol. 192, p. 106585, Jan. 2022, doi: 10.1016/J.COMPAG.2021.106585.
- [22] N. Hassan, S. Ullah, N. Bhatti, H. Mahmood, and M. Zia, "The Retinex based improved underwater image enhancement," *Multimed Tools Appl*, vol. 80, no. 2, pp. 1839–1857, Jan. 2021, doi: 10.1007/S11042-020-09752-2/METRICS.
- [23] J. Zhou, J. Yao, W. Zhang, and D. Zhang, "Multi-scale retinex-based adaptive gray-scale transformation method for underwater image enhancement," *Multimed Tools Appl*, vol. 81, no. 2, pp. 1811–1831, Jan. 2022, doi: 10.1007/S11042-021-11327-8/METRICS.
- [24] J. Wu, X. Liu, Q. Lu, Z. Lin, N. Qin, and Q. Shi, "FW-GAN: Underwater image enhancement using generative adversarial network with multi-scale fusion," *Signal Process Image Commun*, vol. 109, p. 116855, Nov. 2022, doi: 10.1016/J.IMAGE.2022.116855.
- [25] Y. Huang, F. Yuan, F. Xiao, and E. Cheng, "Underwater image enhancement based on color restoration and dual image wavelet fusion," *Signal Process Image Commun*, vol. 107, p. 116797, Sep. 2022, doi: 10.1016/J.IMAGE.2022.116797.
- [26] W. Zhang, P. Zhuang, H. H. Sun, G. Li, S. Kwong, and C. Li, "Underwater Image Enhancement via Minimal Color Loss and Locally Adaptive Contrast Enhancement," *IEEE Transactions on Image Processing*, vol. 31, pp. 3997–4010, 2022, doi: 10.1109/TIP.2022.3177129.
- [27] C. Li, S. Anwar, J. Hou, R. Cong, C. Guo, and W. Ren, "Underwater Image Enhancement via Medium Transmission-Guided Multi-Color Space Embedding," *IEEE Transactions on Image Processing*, vol. 30, pp. 4985–5000, 2021, doi: 10.1109/TIP.2021.3076367.
- [28] P. Zhuang, J. Wu, F. Porikli, and C. Li, "Underwater Image Enhancement With Hyper-Laplacian Reflectance Priors," *IEEE Transactions on Image Processing*, vol. 31, pp. 5442–5455, 2022, doi: 10.1109/TIP.2022.3196546.
- [29] S. Minaee, Y. Boykov, F. Porikli, A. Plaza, N. Kehtarnavaz, and D. Terzopoulos, "Image Segmentation Using Deep Learning: A Survey," *IEEE Trans Pattern Anal Mach Intell*, vol. 44, no. 7, pp. 3523–3542, Jul. 2022, doi: 10.1109/TPAMI.2021.3059968.
- [30] Z. H. Arif et al., "Comprehensive Review of Machine Learning (ML) in Image Defogging: Taxonomy of Concepts, Scenes, Feature Extraction, and Classification techniques," *IET Image Process*, vol. 16, no. 2, pp. 289–310, Feb. 2022, doi: 10.1049/IPR2.12365.
- [31] D. C. Lepcha, B. Goyal, A. Dogra, and V. Goyal, "Image super-resolution: A comprehensive review, recent trends, challenges and applications," *Information Fusion*, vol. 91, pp. 230–260, Mar. 2023, doi: 10.1016/J.INFFUS.2022.10.007.
- [32] B. Goyal, D. C. Lepcha, A. Dogra, and S. H. Wang, "A weighted least squares optimisation strategy for medical image super resolution via multiscale convolutional neural networks for healthcare applications," *Complex and Intelligent Systems*, vol. 8, no. 4, pp. 3089–3104, Aug. 2022, doi: 10.1007/S40747-021-00465-Z/FIGURES/4.
- [33] S. S. A. Zaidi, M. S. Ansari, A. Aslam, N. Kanwal, M. Asghar, and B. Lee, "A survey of modern deep learning based object detection models," *Digit Signal Process*, vol. 126, p. 103514, Jun. 2022, doi: 10.1016/J.DSP.2022.103514.
- [34] Z. Jiang, Z. Li, S. Yang, X. Fan, and R. Liu, "Target Oriented Perceptual Adversarial Fusion Network for Underwater Image Enhancement," *IEEE Transactions on Circuits and Systems for Video Technology*, vol. 32, no. 10, pp. 6584–6598, Oct.

- 2022, doi: 10.1109/TCSVT.2022.3174817.
- [35] P. Lin, Y. Wang, G. Wang, X. Yan, G. Jiang, and X. Fu, "Conditional generative adversarial network with dual-branch progressive generator for underwater image enhancement," *Signal Process Image Commun*, vol. 108, p. 116805, Oct. 2022, doi: 10.1016/J.IMAGE.2022.116805.
- [36] Z. Huang, J. Li, Z. Hua, and L. Fan, "Underwater Image Enhancement via Adaptive Group Attention-Based Multiscale Cascade Transformer," *IEEE Trans Instrum Meas*, vol. 71, 2022, doi: 10.1109/TIM.2022.3189630.
- [37] Z. Al-Ameen, "Expeditious Contrast Enhancement for Grayscale Images Using a New Swift Algorithm," *Statistics, Optimization & Information Computing*, vol. 6, no. 4, pp. 577–587, Nov. 2018, doi: 10.19139/SOIC.V6I4.436.
- [38] E. Provenzi, L. De Carli, A. Rizzi, and D. Marini, "Mathematical definition and analysis of the Retinex algorithm," *JOSA A*, Vol. 22, Issue 12, pp. 2613–2621, vol. 22, no. 12, pp. 2613–2621, Dec. 2005, doi: 10.1364/JOSAA.22.002613.
- [39] Y. Zou, X. Dai, W. Li, and Y. Sun, "Robust design optimisation for inductive power transfer systems from topology collection based on an evolutionary multi-objective algorithm," *IET Power Electronics*, vol. 8, no. 9, pp. 1767–1776, Sep. 2015, doi: 10.1049/IET-PEL.2014.0468.
- [40] Łoza, D. R. Bull, P. R. Hill, and A. M. Achim, "Automatic contrast enhancement of low-light images based on local statistics of wavelet coefficients," *Digit Signal Process*, vol. 23, no. 6, pp. 1856–1866, Dec. 2013, doi: 10.1016/J.DSP.2013.06.002.
- [41] G. Hou, Z. Pan, B. Huang, G. Wang, and X. Luan, "Hue preserving-based approach for underwater colour image enhancement," *IET Image Process*, vol. 12, no. 2, pp. 292–298, Feb. 2018, doi: 10.1049/IET-IPR.2017.0359.
- [42] R. C. Gonzalez and R. E. Woods, "Digital Image Processing," 2008.
- [43] "Effective color displays : theory and and practice : Travis, David : Free Download, Borrow, and Streaming : Internet Archive." <https://archive.org/details/effectivecolordi0000trav> (accessed Jun. 08, 2023).
- [44] V. Oppenheim, R. W. Schafer, R. W. Schafer, and T. G. Stockham, "Nonlinear Filtering of Multiplied and Convolved Signals," *IEEE Transactions on Audio and Electroacoustics*, vol. 16, no. 3, pp. 437–466, 1968, doi: 10.1109/TAU.1968.1161990.
- [45] D. C. Lepcha, B. Goyal, A. Dogra, S. H. Wang, and J. S. Chohan, "Medical image enhancement strategy based on morphologically processing of residuals using a special kernel," *Expert Syst*, p. e13207, 2022, doi: 10.1111/EXSY.13207.
- [46] C. Li et al., "An Underwater Image Enhancement Benchmark Dataset and beyond," *IEEE Transactions on Image Processing*, vol. 29, pp. 4376–4389, 2020, doi: 10.1109/TIP.2019.2955241.
- [47] Nair, K. S. S. . (2023). Rapidly Convergent Series from Positive Term Series. *International Journal on Recent and Innovation Trends in Computing and Communication*, 11(3), 79–86. <https://doi.org/10.17762/ijritcc.v11i3.6204>
- [48] Miller, J., Evans, A., Martinez, J., Perez, A., & Silva, D. Predictive Maintenance in Engineering Facilities: A Machine Learning Approach. *Kuwait Journal of Machine Learning*, 1(2). Retrieved from <http://kuwaitjournals.com/index.php/kjml/article/view/113>
- [49] Juneja, V., Singh, S., Jain, V., Pandey, K. K., Dhabliya, D., Gupta, A., & Pandey, D. (2023). Optimization-based data science for an IoT service applicable in smart cities. *Handbook of research on data-driven mathematical modeling in smart cities* (pp. 300-321) doi:10.4018/978-1-6684-6408-3.ch016 Retrieved from www.scopus.com